Research Square

Preprints are preliminary reports that have not undergone peer review.
They should not be considered conclusive, used to inform clinical practice,
or referenced by the media as validated information.

Investigation of Deformation in Metal Additively Manufactured Automotive Components Using Different 3D Scanning Methods

Valentin Endre Szabó

szabo.valentin@nje.hu

John von Neumann University

Adrián Bognár

John von Neumann University

Zoltán Weltsch

Széchenyi István University

Research Article

Keywords: 3D Metal printing, Additive manufacturing, Metal additive manufacturing, 3D Scanning, Point cloud, Dimensional inspection

Posted Date: August 11th, 2026

DOI: https://doi.org/10.21203/rs.3.rs-10495235/v1

License: This work is licensed under a Creative Commons Attribution 4.0 International License.
Read Full License

Additional Declarations: No competing interests reported.

Abstract

Geometric inspection of parts produced by metal additive manufacturing is of paramount importance, as temperature differences during the manufacturing process can cause internal residual stresses, global deformation, and local shape deviations. In this study, two optical 3D scanning approaches based on different acquisition principles were compared: an automated robot-assisted structured-light system and a handheld blue-laser scanning system. The aim was to examine their applicability and practical limitations in identifying and quantifying the geometric characteristics of a deformed metal additively manufactured component. The dataset acquired by the automated structured-light system was used as the comparison reference. A twin-cantilever test specimen made of 1.2709-grade tool steel was investigated after one side had been partially separated from the base plate using wire electrical discharge machining. The datasets were aligned using a local best-fit procedure based on three planar surfaces of the base plate, followed by full-surface and local deviation analyses. The automated structured-light measurement comprised 1,733,820 surface points, whereas the handheld laser measurement comprised 617,913 surface points. Both approaches represented the global deformation pattern similarly, and the flatness of the upper surface was 0.51 mm and 0.52 mm, respectively. The largest deviations were concentrated around edges, corners, and small geometric details. The handheld laser scanning approach was suitable for identifying global deformation patterns, while the automated structured-light system provided a denser and more detailed representation of fine local features.

1. Introduction & Literature Review

1.1. Metal additive manufacturing in the automotive industry

Today, additive manufacturing has evolved into one of the new manufacturing techniques with the greatest potential. Techniques previously used for rapid prototyping are increasingly suitable for the production of functional parts as well [1]. Metal 3D printing techniques, particularly powder-bed fusion (PBF) additive manufacturing techniques, hold great potential. The best-known of these are direct metal laser sintering (DMLS) and selective laser melting (SLM), which enable the production of nearly dense metal structures with minimal material loss. They enable the design and manufacture of parts with complex, intricate geometries, thereby pushing the boundaries of design and providing engineers with a high degree of freedom [2][10]. Unlike traditional machining and forming processes, in additive manufacturing, the part is built up layer by layer based on a digital model [3]. This layer-by-layer manufacturing process ensures geometric freedom and enables the production of complex parts that would be difficult, uneconomical, or impossible to manufacture using traditional technologies [4] [7]. These advantages and possibilities are becoming increasingly important in the automotive industry, in the world of limited-edition supercars, in motorsports, in custom vehicle manufacturing, and in drone production, where every gram counts [5] [8–9]. In the future, metal 3D printing may play an important role in additional fields where weight reduction (e.g., the space industry, the aircraft industry, and drone

manufacturing), functional integration, rapid product development, and adaptation to specific needs are all critical factors [6] [7].

Metal additive manufacturing processes can be classified into several technological groups, one of the most widespread of which is laser powder bed fusion [5]. In this process, a focused laser beam selectively melts the metal powder based on the layer-by-layer cross-section of a three-dimensional computer model [6]. During the process, successive layers build up to form the finished part. The technology is suitable for processing, among other materials, stainless steels, aluminum alloys, titanium alloys, nickel-based alloys, and maraging steels [7]. Initially, the automotive industry used additive manufacturing primarily to produce visual models, form-verification prototypes, casting patterns, and manufacturing aids. In recent years, however, it has played an increasingly important role in the production of functional prototypes, custom parts, lightweight structural elements, thermal management components, tools, and low-volume replacement parts [10]. By combining additive manufacturing with topological optimization, material can be placed primarily in those areas where it is actually necessary for load transfer [11]. This makes it possible to reduce the weight of components without compromising the required mechanical load-bearing capacity [12]. Another advantage is the integration of structures that were previously assembled from multiple parts into a single component. Combining components can reduce the number of joints, fasteners, assembly operations, and potential failure points. This simplifies assembly operations on automotive production lines, resulting in significant reductions in manufacturing costs [12] [13]. In addition, it can accelerate the development process, as geometric modifications do not require the manufacture of new forming or casting tools; instead, they can be built onto existing tools or components. This approach can be applied during repairs or redesigns in any area of the manufacturing sector.

At the same time, additive manufacturing cannot be considered a general substitute for traditional mass production technologies; when used appropriately, it rather complements them and makes them more efficient. Its industrial application may be limited by lower productivity, high raw material and equipment costs, the need for post-processing, surface quality, and issues related to process repeatability and certifiability [14]. The cost-effectiveness of the technology depends largely on the part’s size, geometric complexity, production volume, the need for post-processing, and the extent to which additive manufacturing can reduce the number of assembly or manufacturing steps. Consequently, metal additive manufacturing is particularly advantageous for parts that have complex or optimized geometries, a high degree of functional integration, are produced in small batches, or offer high added value relative to their size [15].

The quality of automotive components is fundamentally determined not only by the mechanical properties of the material but also by dimensional and geometric accuracy. Components must meet requirements regarding assembly, load transfer, fit, sealing, vibration behavior, and service life [16]. Deviations from the nominal geometry can adversely affect performance even if the material itself meets the specified strength requirements. Therefore, geometric inspection is of great importance in the quality assurance of parts produced by metal additive manufacturing, and there are currently no regulations or

standards governing this area. This is currently one of the obstacles to the wider industrial adoption of this technology. Ensuring geometric accuracy poses a major challenge in laser-based powder-bed metal printing, as the part is subjected to repeated, highly localized heating and cooling cycles during manufacturing. The resulting temperature differences can cause residual stresses, shrinkage, warping, and local shape deviations.

For all these reasons, the conformity of automotive parts manufactured using metal additive manufacturing cannot be assessed solely on the basis of nominal technological parameters or the original CAD model. Reliable dimensional and geometric inspection is required, capable of identifying the overall warpage and local geometric deviations of the entire part. Traditional measurement methods may be suitable for examining individual dimensions or easily accessible geometric features, but they can provide only limited information about complex free-form surfaces and spatially distributed deformations; surface scanning is better suited for this purpose [17] [18].

1.2. The Role of 3D Surface Scanning in Geometric Inspection in Metal Additive Manufacturing

Full-surface optical 3D scanning enables the non-contact digitization of most of a part, followed by a comparison of the measured geometry with a nominal CAD model or another set of measurement data. This data can be stored and represents the entire part; furthermore, these 3D scanners are well known and widely used in today's automotive production lines and quality control processes. They are also suitable for identifying global distortions, local shape deviations, and characteristic deformation patterns, as these cannot always be adequately described based on a few conventional dimensions or a limited number of measurement points. A spatial examination of the entire geometry is particularly necessary for complex, free-form, or thin-walled parts [19].

The advantage of optical 3D scanning is that it allows for the collection of large amounts of surface data in a short amount of time using a non-contact method. The point cloud or polygon mesh generated as a result of the measurement allows for the examination of the workpiece's entire surface, comparison with the nominal CAD geometry, and the visualization of deviations using a color map. This makes it possible to determine not only the magnitude of the deviation but also its spatial location and distribution. The method is suitable for identifying global warps, local protrusions, depressions, waviness, and other characteristic deformation patterns. In addition, it can be used to measure traditional mechanical engineering dimensional tolerances or form tolerances based on point clouds; however, in this case, an additional advantage is that an order of magnitude more measurement points are available. Another advantage of full-surface measurement data is that various geometric characteristics—such as flatness, cylindricity, circularity error, diameter, or surface deviation—can be determined from the same dataset [20].

However, the reliability of measurement results is significantly influenced by the scanning principle of the scanner used, its spatial resolution, point spacing, calibration, data acquisition strategy, and subsequent point cloud and mesh processing. Different 3D scanning systems can therefore yield varying point

densities, noise levels, surface coverage, and geometric results for the same part [21]. Industrial, automated optical measurement systems can provide high repeatability and detailed surface data, while the main advantages of handheld scanners are mobility, flexible applicability, and rapid data collection. Consequently, when evaluating the deformation of parts manufactured using metal additive manufacturing, it is necessary to consider not only the measured geometric deviations but also the characteristics of the measurement system used. Comparing datasets from 3D scanners operating on different measurement principles makes it possible to determine the accuracy and level of detail with which each system can identify global and local deformations, as well as the quality control or engineering tasks for which they can be reliably applied [20].

For these reasons, the aim of this study is to examine the measurement capabilities, accuracy, and practical limitations of various 3D scanning systems when used with metal-printed parts that have a dominant dimension in one direction.

2. Methodology

2.1. The Test Specimens and the Scanning Environment

For the measurements, we used test specimens with a twin-cantilever geometry, which, due to their design, are suitable for illustrating the stresses generated during metal additive manufacturing through the appearance of dramatic deformations. We compare the test specimens in their cut, already deformed state—not to the CAD model, but to each other. The part was produced on an EOSINT M270 metal additive manufacturing system. The material is martensitic hardenable tool steel, designated 1.2709. After printing, one side of the workpiece was removed from the build plate using wire electrical discharge machining (WEDM), which is a sufficiently precise and controlled process. It also effectively minimizes the potential for additional internal stresses induced by thermal effects. The geometry of the test specimen is shown in Fig. 1.

The role and properties of the test specimen’s base plate in this research are multifaceted. On the one hand, they facilitate the alignment of the point cloud with the large, regular, flat surfaces. On the other hand, it contains residual material from previous additions, which is irregular; thus, when aligning the point cloud, these provide valuable feedback on the accuracy of the mesh alignment—larger deviations are likely to be detected on these surfaces in the event of an inaccurate alignment. Furthermore, the test specimen is not centered on the base plate; this placement also facilitates alignment, as the asymmetrically positioned test specimen can only be aligned in one way (just as in real-world assembly tasks). In addition, there is a groove on one side of the base plate, so the scanned surface contains unique features that can be used to verify the fit.

2.2. Optical 3D measurement systems and software used

For the experiments, two optical 3D scanning approaches based on different acquisition principles and application concepts were compared. The reference dataset was acquired using an automated, robot-

assisted structured blue-light stereo scanning system (GOM ATOS Q 12M), while the comparative dataset was acquired using a handheld blue-laser line scanning system (SHINING 3D FreeScan UE11). Hereafter, these are referred to as the automated structured-light system and the handheld laser system, respectively. The comparison was based on the point cloud captured by GOM, and we used Zeiss INSPECT Optical 3D software for the comparison.

The automated structured-light system is a stereo-camera-based optical measurement system that uses a structured blue-light pattern. During measurement, the projector projects a specific light pattern onto the surface being inspected, which is captured by two high-resolution cameras. The system is capable of capturing up to 12 million surface measurement points from a single measurement position. Depending on the measurement volume used, the point spacing can be adjusted between 0.03 and 0.12 mm, enabling detailed surface measurement of small- and medium-sized parts with complex geometries. The measurement head used in this research operates as part of an automated measurement system mounted on a robotic arm in a controlled measurement laboratory environment. Robotic data acquisition is performed based on predefined measurement positions and a measurement program, thereby reducing the direct influence of the operator and improving the repeatability of the measurement process. Structured-light systems of this type can be used in manual, semi-automatic, and fully automated configurations and are suitable for serial industrial quality control tasks, full-surface nominal-actual comparisons, and the evaluation of geometric and shape deviations.

In contrast, the handheld laser scanning system uses blue laser lines and is moved continuously around the investigated component by the operator. During the measurement, the operator continuously moves the device around the part, while the system generates a point cloud based on the laser lines projected onto the surface. Typically, reference markers placed on the workpiece help align the various measurement positions. Manual data acquisition provides a high degree of flexibility; however, the measurement results can be significantly influenced by the scan path chosen by the operator, the device's speed of movement, the working distance, the direction of approach to the surface, and the placement of the reference markers. Due to the small size of the specimen, no separate scanning sessions had to be merged during post-processing. The handheld laser system has an adjustable point spacing of 0.05–3 mm; therefore, its maximum achievable spatial resolution is theoretically lower than that of the the automated structured-light system. A larger point spacing results in sparser surface sampling, which can lead to information loss or greater deviation, particularly when examining small details, edges, local protrusions, and subtle shape variations. However, point spacing primarily characterizes spatial resolution and therefore cannot be considered a direct indicator of measurement accuracy on its own. The actual measurement result is influenced not only by the instrument's accuracy but also by calibration, surface properties, data acquisition strategy, registration, and post-processing. Due to its portability and ease of handheld operation, the handheld blue laser scanner is particularly advantageous for tasks where transporting the workpiece to a measurement laboratory is difficult, or where fast and flexible on-site digitization is required. Typical applications include reverse engineering, reconstructing CAD models of existing parts, supporting repair and redesign tasks, and performing geometric analysis of competitor or previously undocumented products. The system may also be

suitable for on-site surveying of larger parts, machine components, and industrial equipment, as well as for creating geometric models needed for simulation. The manufacturer's application examples also primarily feature reverse engineering, repair, and design tasks that require portability. Figure 2 shows the data captured by the scanner.

Figure 3 illustrates the two different data acquisition configurations used in the study.

3. Results & Discussion

The automated structured-light measurement contained 1,733,820 surface points, while the handheld laser measurement contained 617,913 surface points. The datasets were aligned using a local best-fit procedure based on the three largest planar surfaces of the base plate. The captured data is shown in Fig. 4.

During the evaluation, the assessment criteria were as follows. We examined the extent of geometric discrepancies between the point clouds and triangulated surfaces generated by the automated structured-light and handheld laser scanning systems, as well as whether these discrepancies are distributed evenly across the examined surfaces or concentrated in specific geometric regions. We also analyzed how differences in point density, surface coverage, and measurement noise affect the identified deformations. We paid particular attention to the extent to which data from the two measurement systems yield similar global geometric characteristics. Finally, we evaluated whether the handheld laser scanning approach could be suitable for preliminary geometrical inspection and deformation analysis for preliminary geometric inspection and deformation analysis of automotive parts manufactured using metal additive manufacturing. During the evaluation, we performed surface comparisons and color mapping analyses. Figure 4 shows a comparison of the raw data.

Figure 4(a) shows the dataset acquired using the handheld laser scanning system; we have filled in the gaps and the missing area along the cut. These areas are not included in the evaluation; they were used solely to increase contrast. Figure 4(b) shows the reference dataset acquired using the automated structured-light system. Figure 4(c) shows the surfaces after alignment, which served as the basis for the evaluation. Here, differences resulting from the resolution of the two scanners are already observable, particularly along the edges. Figure 4(d) was created using the state shown in Fig. 4(c); there, deviations along the centerline can be observed. Based on these, it can be stated that the main, global deformation pattern and the surfaces used as a baseline are nearly identical; deviations can only be observed along the positive and negative corners. The results of the surface comparison are presented in Fig. 5.

Figure 5(a) visually illustrates the differences between the joined surfaces, while Fig. 5(b) shows the surface deviations relative to the structured-light reference dataset. Figure 5(c) highlights the area of the color map that exhibits the greatest deviations and contains the finest details. Figure 5(d) provides guidance for interpreting this. Here, we can see that the reference surface, shown in red, provides a sharper and more detailed representation of the corner regions; this is also supported by Fig. 5(b), where

the color map shows good agreement across the entire surface of the test specimen on large areas, with the exception of the edges. We examined the edges of the test specimen using a cross-section along its centerline, as shown in Fig. 6.

Figure 6 shows the differences between the two data sets that form along the edges, confirming the findings observed in the previously highlighted section (Fig. 5c). These variations along the edges can be attributed to the distance between measurement points and the resolution. These are fundamentally justified by the scanners' different intended uses. In contrast, the global deviations were in good agreement; however, on larger surfaces, the surface measured and polygonized using the handheld laser scanning system was in every case a few hundredths of a millimeter larger, and generally only the surface structure stood out from the reference surface (Fig. 5a and b). This can be explained by the larger polygons resulting from the resolution and the distance between measured points—which also cause rounding along the edges—as well as by the thickness of the matting spray used to aid scanning. The flatness of the upper surface was 0.51 mm based on the automated structured-light dataset and 0.52 mm based on the handheld laser dataset, corresponding to an absolute difference of 0.01 mm.

Based on the data above, however, it can be concluded that the scanned data shows good agreement; the magnitude and nature of the global deviations are also consistent, so the data digitized with the SHINING scanner are also suitable for detecting global deformation patterns. However, the automated structured-light system was more suitable for examining sharp edges and small geometric features because its smaller point spacing enabled a denser representation of these regions than the handheld laser system.

4. Summary & Conclusions

In this study, we examined a twin-cantilever test specimen—manufactured using metal additive manufacturing and deformed following partial base plate separation—using two optical 3D scanning systems based on different operating principles. The automated structured-light measurement contained 1,733,820 surface points, whereas the handheld laser measurement contained 617,913 surface points. We aligned the two datasets using a local best-fit method based on the three large flat surfaces of the test specimen's base plate.

Based on the results, the two measurement systems represented the test specimen's global geometry and main deformation pattern in nearly identical ways. The flatness of the upper surface was 0.51 mm based on the automated structured-light dataset and 0.52 mm based on the handheld laser dataset, meaning the difference between the global geometric characteristics was only 0.01 mm. This supports the assumption that the handheld scanner may be suitable for detecting larger deformations and global deformation trends.

The more significant differences were not evenly distributed across the examined surface but were concentrated primarily around edges, corners, and small geometric details. The handheld laser dataset's lower point count and larger point spacing and greater available point spacing resulted in sparser

surface sampling and larger polygons, which led to the smoothing of sharp transitions and a less accurate representation of local details. On large, nearly flat surfaces, however, only a deviation of a few hundredths of a millimeter was observed. In addition to the resolution, the thickness of the matte coating may have contributed to this.

Within the investigated measurement configuration, the handheld laser scanning approach was suitable for identifying the global deformation pattern of the metal additively manufactured specimen. However, the automated structured-light system provided a denser and more detailed surface representation, particularly around sharp edges, corners, and small geometric features. Consequently, the handheld approach may be applied for preliminary geometrical inspection, reverse engineering, and the evaluation of larger deformation trends, while the automated structured-light approach is preferable when high repeatability and the detailed characterization of local geometrical deviations are required.

Declarations

Ethics, Consent to Participate, and Consent to Publish declarations

not applicable.

Author Contribution

Conceptualization, V.E.S. and Z.W.; methodology, V.E.S., A.B. and Z.W.; investigation, V.E.S. and A.B.; automated structured-light data acquisition, V.E.S. and A.B.; handheld laser data acquisition and polygonization, A.B.; software and data processing, V.E.S. and A.B.; point-cloud registration and surface comparison, V.E.S.; validation, V.E.S. and Z.W.; formal analysis and interpretation of the results, V.E.S., A.B. and Z.W.; data curation, V.E.S. and A.B.; visualization and figure preparation, V.E.S. and Z.W.; writing—original draft preparation, V.E.S.; writing—review and editing, Z.W.; supervision, Z.W. All authors reviewed and approved the final version of the manuscript.

Acknowledgements

This research was supported by the University Research Scholarship Programme (EKÖP) of the Ministry of Culture and Innovation, funded by the National Research, Development and Innovation Fund.

Data Availability

The datasets generated during and/or analysed during the current study are available from the corresponding author on reasonable request.

References

1. Markovits T, Szederkényi B. Investigation of generative design for powder bed fusion technology in case of Formula Student race car components using Ti6Al4V alloy. J Manuf Process. 2022;80:220–31. 10.1016/j.jmapro.2022.05.058.
2. Hunar M, Jancar L, Krzikalla D, Kaprinay D, Srnicek D. Comprehensive view on racing car upright design and manufacturing. Symmetry. 2020;12(6):1020. https://doi.org/10.3390/sym12061020.
3. Choudhuri B, Uddin MF, Sen R. (2026). Review on 3D printing technology in automotive industry and electric vehicle. *Proceedings of the Institution of Mechanical Engineers, Part D: Journal of Automobile Engineering*, *240*(5), 2325–2345. https://doi.org/10.1177/09544070251337273
4. Milewski JO. Additive Manufacturing Metal, the Art of the Possible. Additive Manufacturing of Metals. Springer Series in Materials Science. Volume 258. Cham: Springer; 2017. https://doi.org/10.1007/978-3-319-58205-4_2.
5. Jhinkwan A, Kalsi S, Pankaj P. (2023, February). An overview on 3D metal printing technology in automobile industry. In *AIP Conference Proceedings* (Vol. 2558, No. 1, p. 020028). AIP Publishing LLC. https://doi.org/10.1063/5.0120028
6. Ibraim AS, Absadykov BN. (2024). 3D-printing in the automotive industry. *Bulletin of LN Gumilyov Eurasian National University Technical Science and Technology Series*, *148*(3), 206–218. https://doi.org/10.32523/2616-7263-2024-148-3-206-218
7. Harland D, Alshaer AW, Brooks H. An experimental and numerical investigation of a novel 3D printed sandwich material for motorsport applications. Procedia Manuf. 2019;36:11–8. https://doi.org/10.1016/j.promfg.2019.08.003.
8. Kun K, Török ÁI. 3D digitalizálás ipari drón segítségével= 3D Digitalization with Industrial Drone. GRADUS. 2021;8(1):235–41. https://doi.org/10.47833/2021.1.ENG.003.
9. Kun K, Léder D. Napelemek vizsgálata pilóta nélküli légijárműre integrált kompakt hőkamera segítségével= Measurements on Solar Panels with Drone Mounted Compact Thermal Camera. GRADUS. 2021;8(1):278–85. https://doi.org/10.47833/2021.1.ENG.009.
10. Kun K. Reconstruction and development of a 3D printer using FDM technology. Procedia Eng. 2016;149:203–11. https://doi.org/10.1016/j.proeng.2016.06.657.
11. Mohanavel V, Priyadharshan R, Ravichandran M. The role and application of 3D printer in the automobile industry. ECS Trans. 2022;107(1):12001. 10.1149/10701.12001ecst.
12. Lim CWJ, Le KQ, Lu Q, Wong CH. An overview of 3-D printing in manufacturing, aerospace, and automotive industries. IEEE Potentials. 2016;35(4):18–22. 10.1109/MPOT.2016.2540098.
13. Imeri A, Russell N, Rust J, Sahin S, Fidan I. (2017, June). Maker: 3D printing as an alternative to fabricate the motorsports parts. In *2017 ASEE Annual Conference Proceedings*.
14. Gadagi B, Lekurwale R. (2021). A review on advances in 3D metal printing. *Materials Today: Proceedings*, *45*, 277–283. 10.1016/j.matpr.2020.10.436

15. Liu B, Wang Y, Lin Z, Zhang T. Creating metal parts by fused deposition modeling and sintering. Mater Lett. 2020;263:127252. https://doi.org/10.1016/j.matlet.2019.127252.
16. Xu Z, Dang Y, Munro P. Knowledge-driven intelligent quality problem-solving system in the automotive industry. Adv Eng Inform. 2018;38:441–57. 10.1016/j.aei.2018.08.013.
17. Babu M, Franciosa P, Ceglarek D. Spatio-Temporal Adaptive Sampling for effective coverage measurement planning during quality inspection of free form surfaces using robotic 3D optical scanner. J Manuf Syst. 2019;53:93–108. 10.1016/j.jmsy.2019.08.003.
18. Mendřický R. (2016, September). Using Contactless Scanning for Quality Control of Automotive Parts. In *Materials Science Forum* (Vol. 862, pp. 324–333). Trans Tech Publications Ltd. https://doi.org/10.4028/www.scientific.net/MSF.862.324
19. Wang R, Law AC, Garcia D, Yang S, Kong Z. Development of structured light 3D-scanner with high spatial resolution and its applications for additive manufacturing quality assurance. Int J Adv Manuf Technol. 2021;117(3):845–62. https://doi.org/10.1007/s00170-021-07780-2.
20. Wieczorowski M, Yago IP, Alejandro PD, Gapiński B, Budzik G, Diering M. (2022, April). Comparison of measurements realized on computed tomograph and optical Scanners for elements manufactured by wire arc additive manufacturing. In *International Scientific-Technical Conference MANUFACTURING* (pp. 127–141). Cham: Springer International Publishing. https://doi.org/10.1007/978-3-031-03925-6_12
21. Kritikos M, Urminsky J, Buransky I. Comparison of optical scanner and computed tomography scan accuracy. Digitizing Production Systems: Selected Papers from ISPR2021, October 07–09, 2021 Online, Turkey. Cham: Springer International Publishing; 2021. pp. 521–30. https://doi.org/10.1007/978-3-030-90421-0_44.

Figures

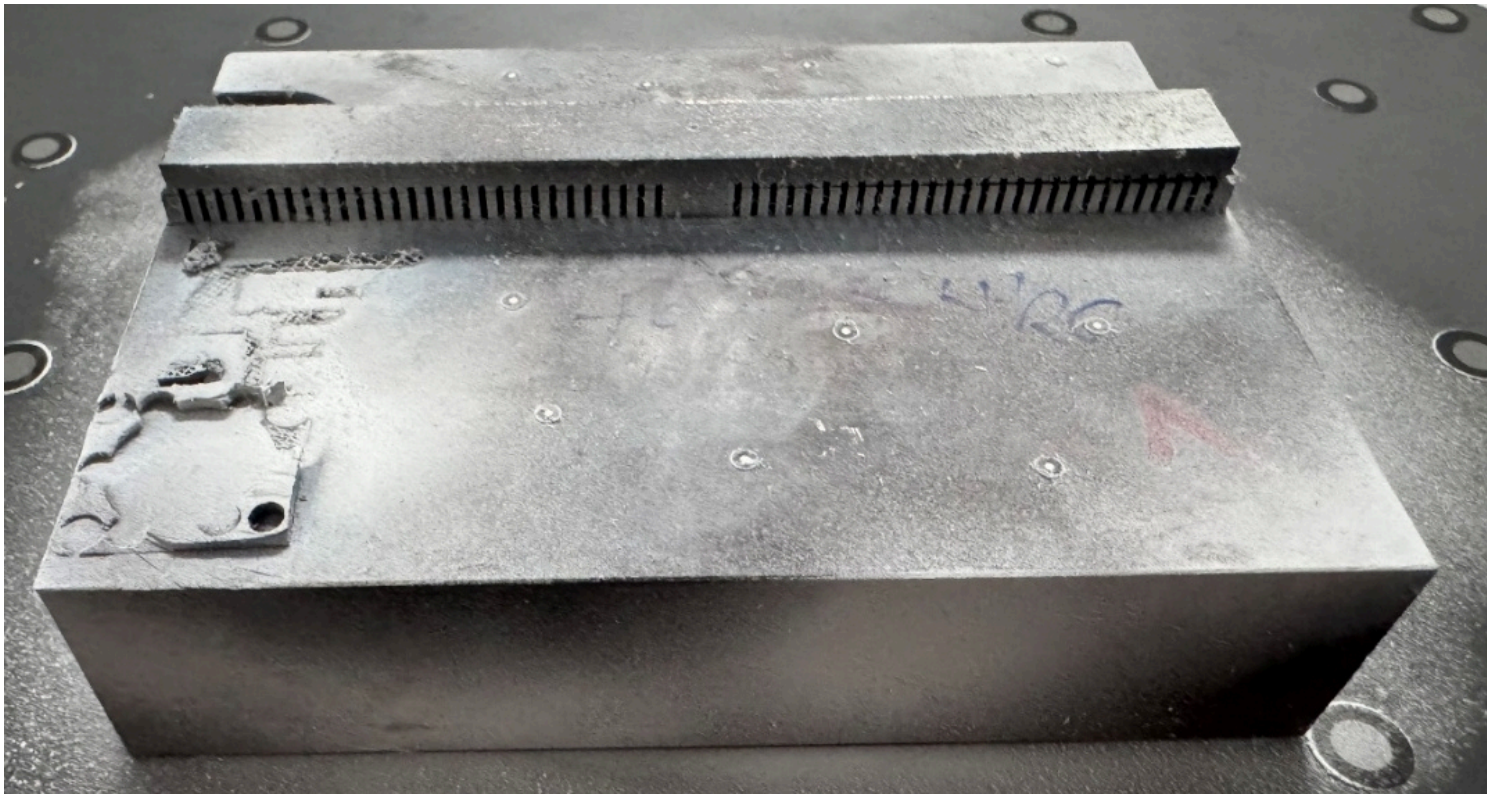


Figure 1

The metal-printed test specimen used, with the matte ink

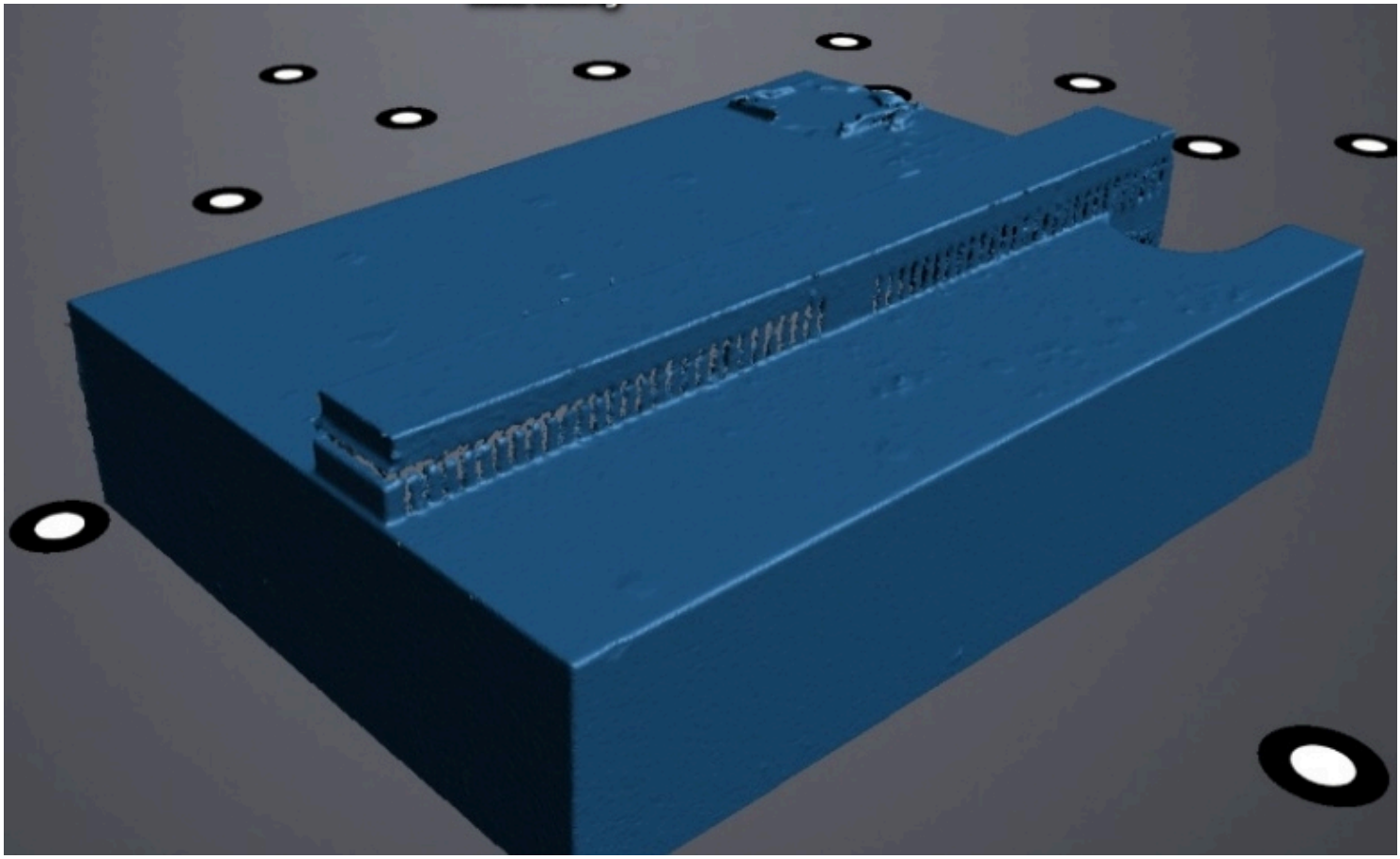


Figure 2

Polygonized surface acquired using the handheld laser scanning system

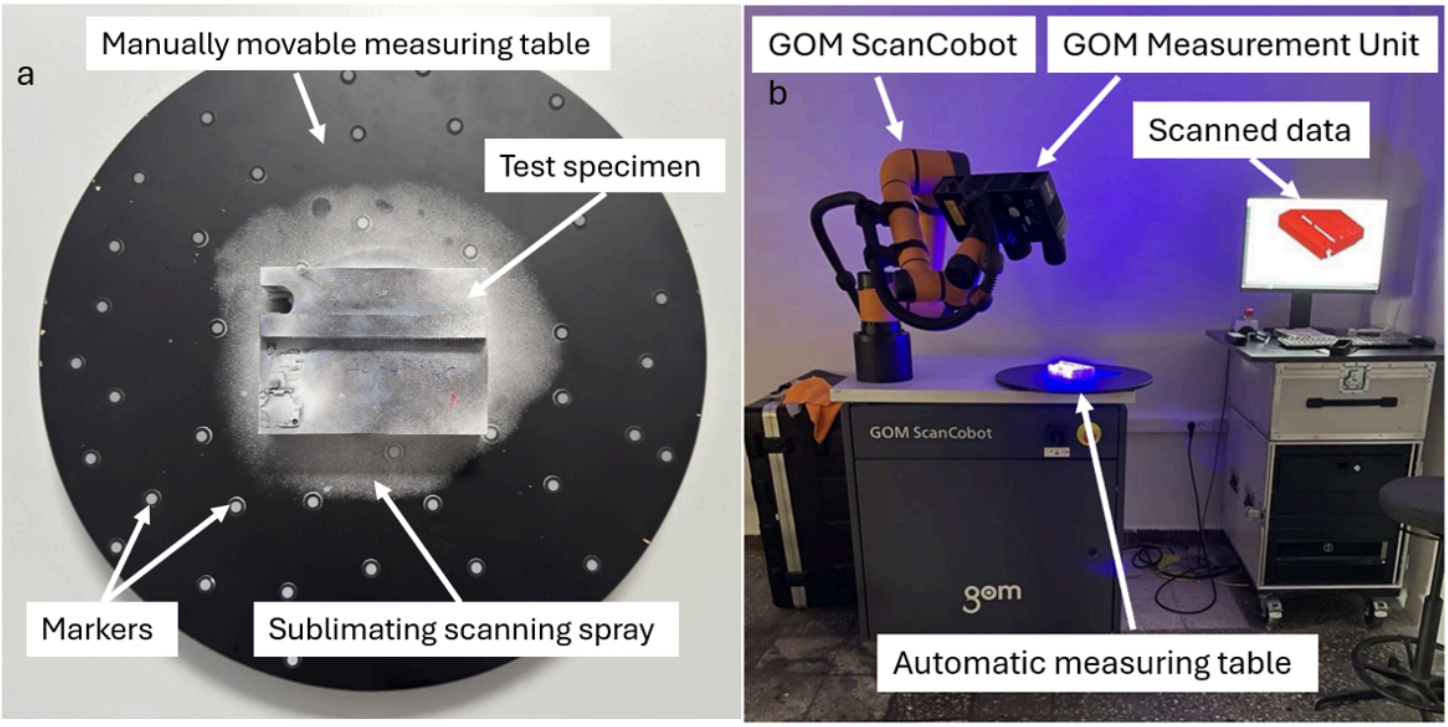


Figure 3

Data acquisition configurations: a) Handheld laser scanning system with a manually movable measuring table; b) Automated structured-light scanning system with a robotic measurement unit

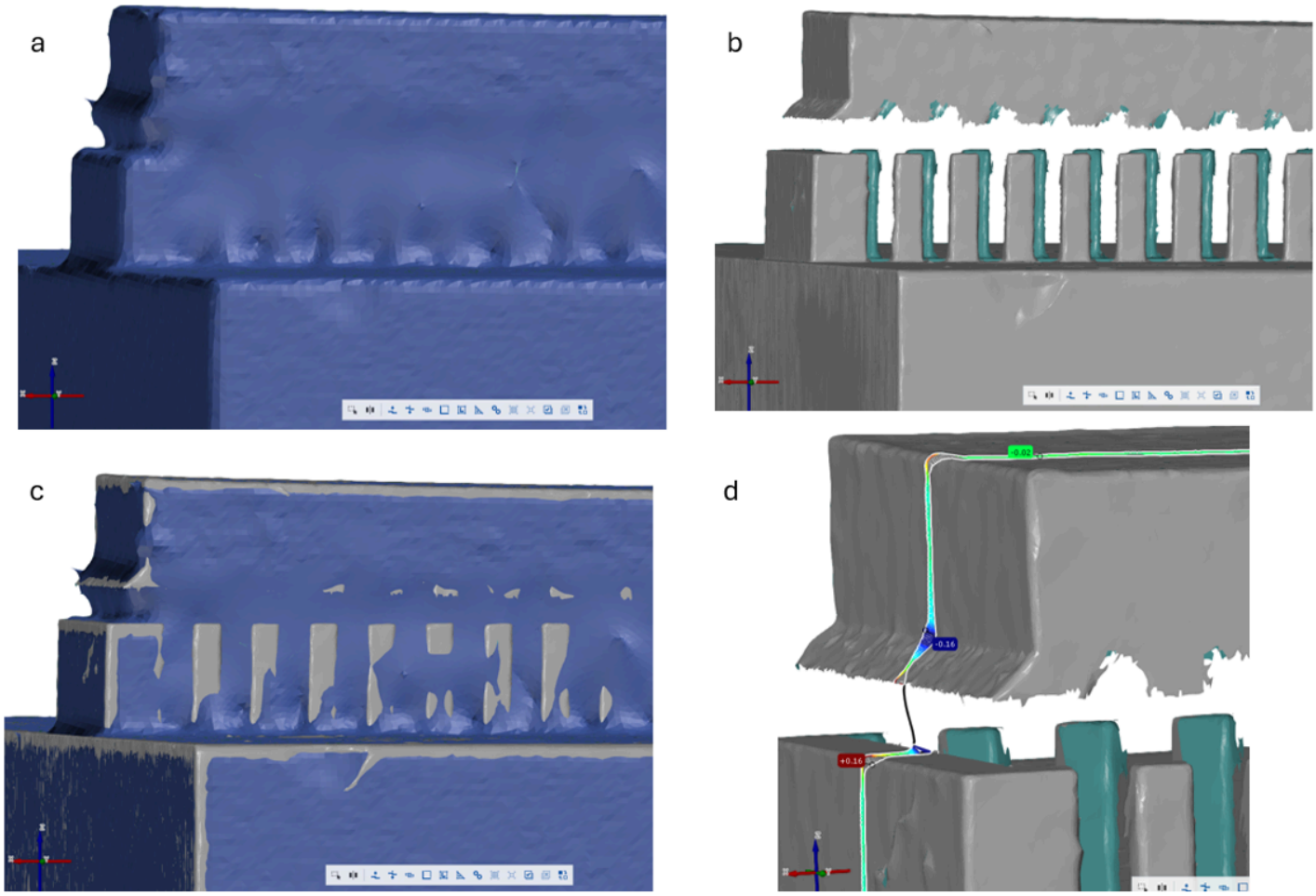


Figure 4

Comparison of the acquired datasets: a) surface acquired using the handheld laser scanning system; b) reference surface acquired using the automated structured-light system; c) surfaces after alignment; d) deviations of the aligned surfaces along the centerline

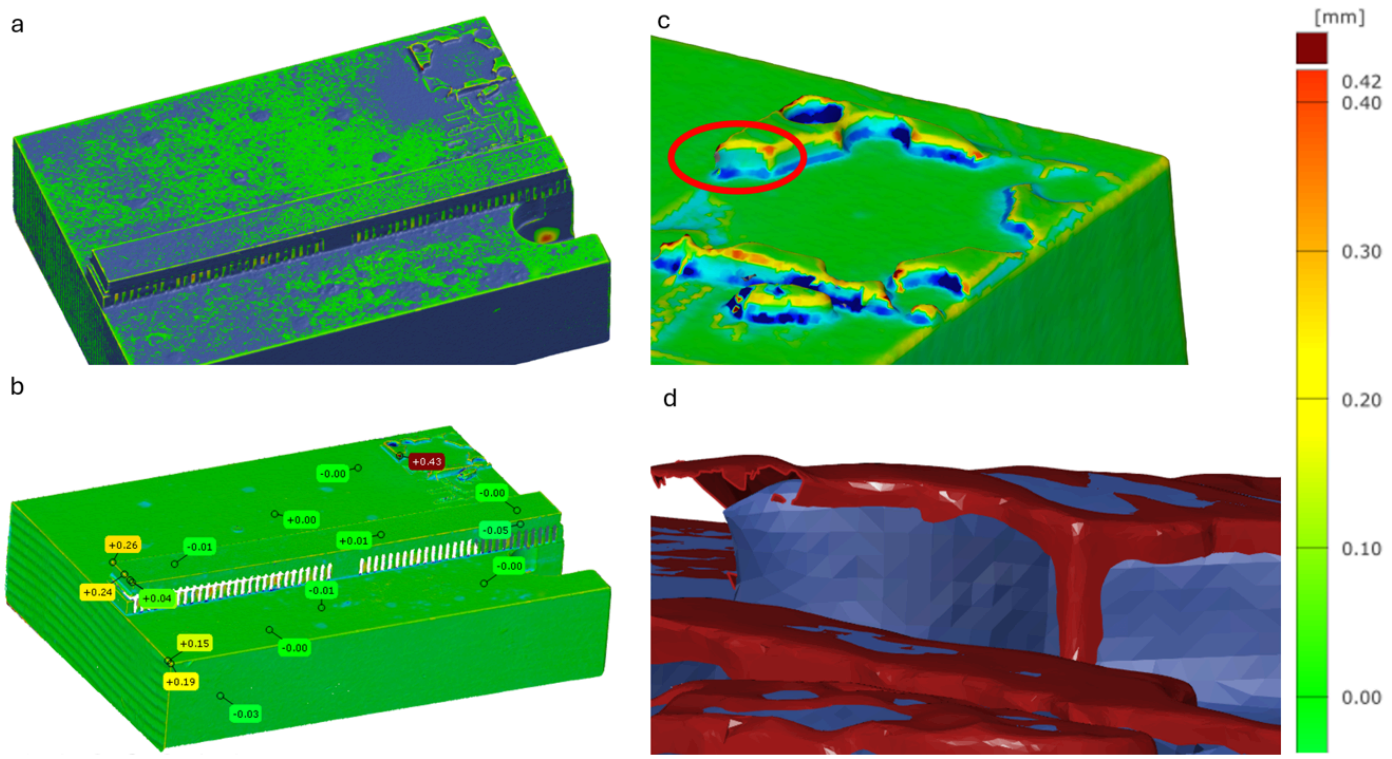


Figure 5

Full-surface comparison of the aligned datasets: a) Visual comparison of the aligned surfaces, with the structured-light reference surface shown in green; b) Color-map representation of the surface deviations; c) Enlarged view of the region containing the largest local deviations; d) Visual interpretation of the differences, with the structured-light reference surface highlighted in red

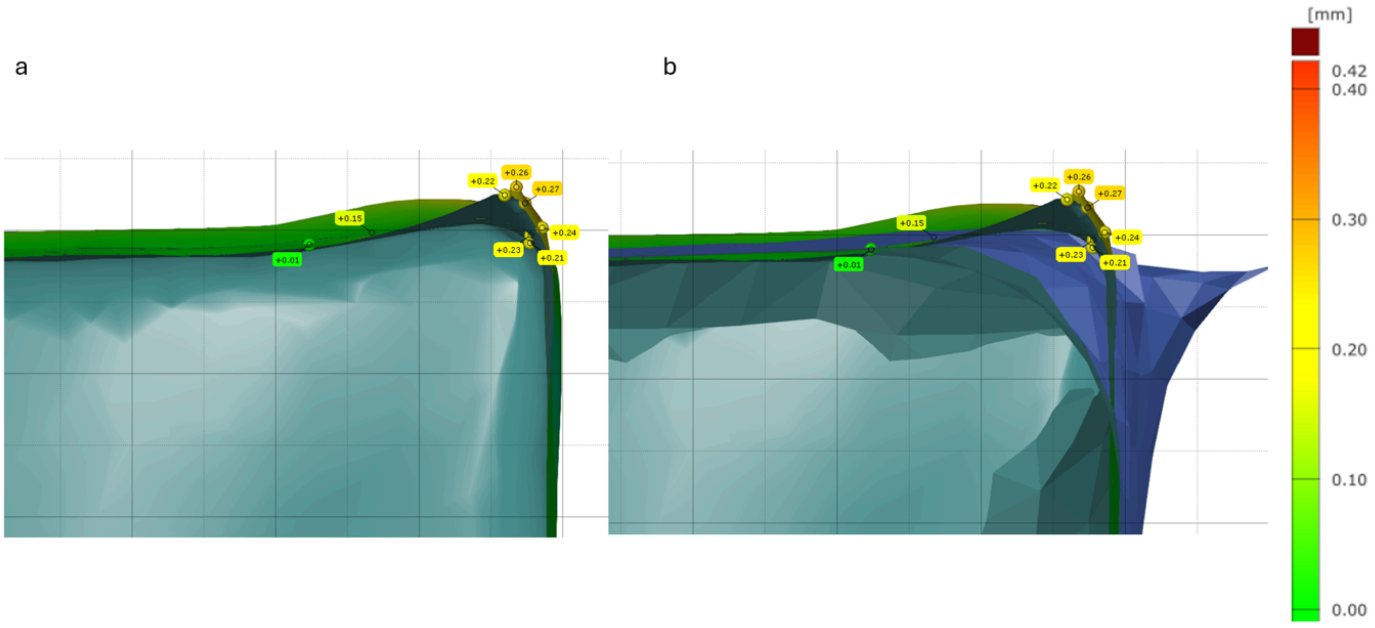


Figure 6

Cross-sectional comparison along the centerline: a) edge-related protrusion represented by the automated structured-light reference dataset; b) deviation of the polygonized surface acquired using the handheld laser system from the reference surface